

# ChemComm

Chemical Communications

Accepted Manuscript

This article can be cited before page numbers have been issued, to do this please use: Y. Qian, J. Chen, C. Shao, X. Wang, J. Gu and H. Zhu, *Chem. Commun.*, 2020, DOI: 10.1039/D0CC00676A.



This is an Accepted Manuscript, which has been through the Royal Society of Chemistry peer review process and has been accepted for publication.

Accepted Manuscripts are published online shortly after acceptance, before technical editing, formatting and proof reading. Using this free service, authors can make their results available to the community, in citable form, before we publish the edited article. We will replace this Accepted Manuscript with the edited and formatted Advance Article as soon as it is available.

You can find more information about Accepted Manuscripts in the [Information for Authors](#).

Please note that technical editing may introduce minor changes to the text and/or graphics, which may alter content. The journal's standard [Terms & Conditions](#) and the [Ethical guidelines](#) still apply. In no event shall the Royal Society of Chemistry be held responsible for any errors or omissions in this Accepted Manuscript or any consequences arising from the use of any information it contains.

## COMMUNICATION

## Imaging of formaldehyde fluxes in epileptic brains with a two-photon fluorescence probe

Received 00th January 20xx,  
Accepted 00th January 20xx

Jian Chen,<sup>a,†</sup> Chenwen Shao,<sup>a,†</sup> Xueao Wang,<sup>a</sup> Jing Gu,<sup>a</sup> Hai-Liang Zhu,<sup>\*a</sup> Yong Qian<sup>\*a, b</sup>

DOI: 10.1039/x0xx00000x

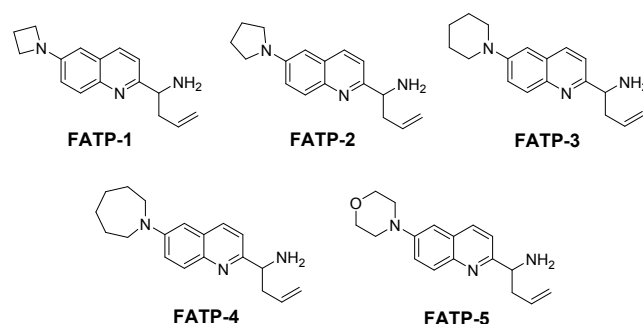
**A two-photon (TP) fluorescence probe has been developed for imaging endogenous FA fluxes during metabolic and epigenetic processes in animal models, especially in live brains.**

Formaldehyde (FA), as a reactive one-carbonyl species, is associated with numerous biochemical processes, including the epigenetic regulation and post-translational modification of proteins.<sup>1</sup> In organisms, FA can be endogenously produced through a series of metabolic processes that catalyzed by demethylases and oxidases, such as lysine-specific demethylase1 (LSD1) and semicarbazide-sensitive amine oxidase (SSAO).<sup>2, 3</sup> After a dynamic process of continuous release and regulation, the physiological steady-state level of FA can reach 0.1 mM in the blood and 0.2-0.4 mM in the normal brain, and the normal levels of intracellular FA are considered to play important roles in human health.<sup>4, 5</sup> However, abnormally elevated FA levels can also cause a variety of disease pathologies.<sup>6-8</sup> Typically, abnormally elevated FA inevitably affects memory, learning, and behavior, and even worse, severe neurological disorders may occur, as a result of the well-established neurotoxicity of FA on the brain.<sup>9</sup> Therefore, developing effective chemical tools for monitoring endogenous FA changes in complex bio-systems, the brain in particular, is conducive to early diagnosis and treatment of related neurodegenerative diseases.

A noninvasive approach for monitoring the FA fluxes in vivo would be ideal. Fluorescent imaging using small-molecule probes is considered as one of the most powerful strategies because of their excellent biocompatibility, high sensitivity, and selectivity.<sup>10</sup> Indeed, a variety of reactivity-based probes have been developed for the specific detection of FA in aqueous solutions, in cells, and in tissues.<sup>11, 12</sup> Despite the great progress, tools for visualizing FA in live brains have yet to be developed. To achieve this, we have to overcome several challenges; the biggest challenge lies in the abilities of these probes to effectively permeate the blood-brain barrier (BBB) and to specifically detect FA in the brain.<sup>13</sup> In addition, we have to take into account the biochemical properties of these small molecules, including cytotoxicity, tissue-penetration depth and

spatiotemporal resolution, as well as their photochemical properties.<sup>14</sup> As such, we turned our attention to two-photon (TP) fluorescence imaging, which is appealing in that it exhibits deeper tissue penetration, higher spatiotemporal resolution, less specimen photo-damage, and less auto-fluorescence interference than one-photon (OP) fluorescence imaging.<sup>15</sup> However, so far, no TP fluorescent probe has been reported for imaging endogenous FA fluxes in live brains. Herein, we report the first two-photon fluorescence probe of its kind capable of monitoring dynamic changes of endogenous FA in the epileptic brains, thus offering a versatile chemical tool for visualizing this reactive carbonyl species in the pathological processes of kainite (KA)-induced epileptic seizure.

Our original design was inspired by quinoline-based brain imaging agents and neuroprotective drugs (Scheme S1).<sup>16, 17</sup> In the design of our probes, the quinoline skeleton was selected as the basic fluorophore due to its extraordinary optical characteristics, including the excellent two-photon excitation properties;<sup>18</sup> in the meantime, the specific homoallylic amine was chosen as the recognition group for FA in our probes following on the reactivity-based sensing mechanism.<sup>19, 20</sup> To further improve the brightness and photostability of the fluorophore while preserving its spectral properties and cell permeability, the electron-donating group was replaced with differently sized nitrogen-containing rings ranging from aziridine to azepane (Scheme 1).<sup>21</sup> On the basis of our hypothesis, these probes themselves should exhibit almost weak fluorescence due to the intramolecular charge transfer (ICT) effect. After de-caging of the specific homoallylamine group by reacting with FA to produce an aldehyde group with the more powerful electron-withdrawing capability, the push-pull electron further heightens, thus yielding the significant fluorescence response.



**Scheme 1.** Chemical structure of two-photon FA fluorescence probes FATP-1~5.

<sup>a</sup> State Key Laboratory of Pharmaceutical Biotechnology, School of Life Sciences, Nanjing University, Xianlin Road 163, Nanjing 210023, China. Email: yongqian@nju.edu.cn or zhuhl@nju.edu.cn

<sup>b</sup> School of Chemistry and Materials Science, Nanjing Normal University, Wenyuan Road 1, Nanjing 210046, China. Email: yongqian@njnu.edu.cn

† J. Chen and C.W. Shao contributed equally to this work.

Electronic Supplementary Information (ESI) available: [details of any supplementary information available should be included here]. See DOI: 10.1039/x0xx00000x

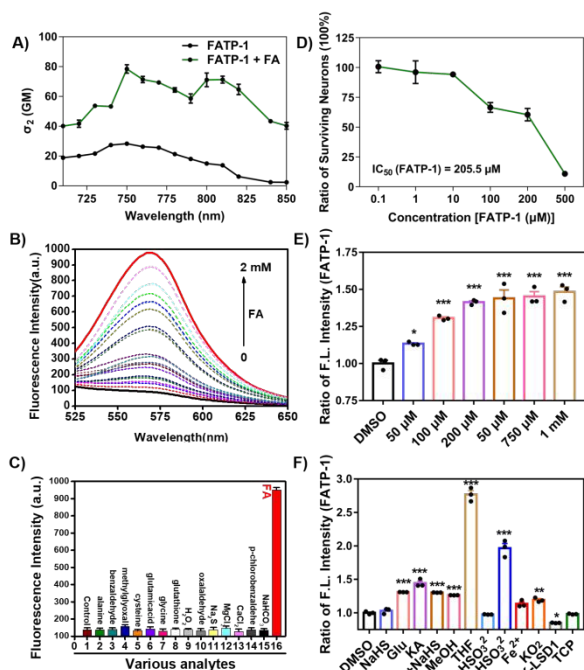


**Figure 1.** (A) Two-photon action spectra of FATP-1 and the corresponding reaction product with formaldehyde (FA) upon excitation from 710 nm to 850 nm. (B) Fluorescence spectra of FATP-1 (20  $\mu\text{M}$ ) after treatment with FA (0–2 mM) in PBS buffer (10 mM, pH 7.4, containing 1% MeCN) for 120 min. (C) The selectivity of FATP-1 (20  $\mu\text{M}$ ) for various relevant analytes (2.0 mM) in PBS buffer (10 mM, pH 7.4, containing 1% MeCN) at 37°C. All the fluorescence data were recorded after 120 min. (D) The cell viability of SH-SY5Y cells treated with different concentrations of FATP-1 (0.1–500  $\mu\text{M}$ ) for 48 h. (E) Fluorescence enhancement of FATP-1 (10  $\mu\text{M}$ , 30 min) after adding different concentrations of FA (0–1000  $\mu\text{M}$ , 4 h) in SH-SY5Y cells. Data were acquired by flow cytometry analysis. Fluorescence excitation: 405 nm, fluorescence emission: 555–651 nm. (F) Fluorescence quantification of SH-SY5Y cells that pre-incubated with or without NaHS (100  $\mu\text{M}$ , 12 h), Glu (2 mM, 12 h), KA (500  $\mu\text{M}$ , 12 h), MeOH (2%, 2 h), THF (10 mM, 2 h), NaHSO<sub>3</sub> (200  $\mu\text{M}$ , 30 min), Fe<sup>2+</sup> (100  $\mu\text{M}$ , 2 h), KO<sub>2</sub> (200  $\mu\text{M}$ , 2 h), GSK-LSD1 (1  $\mu\text{M}$ , 12 h), and TCP (20  $\mu\text{M}$ , 12 h), then treated with FATP-1 (10  $\mu\text{M}$ , 30 min) in the fresh medium for another 30 min before performing flow cytometry analysis. Fluorescence excitation: 405 nm, fluorescence emission: 555–651 nm. The error bars were  $\pm\text{SD}$  (n=3). Statistical analyses performed with an Ordinary one-way ANOVA test to the control with DMSO treatment, \* $P < 0.05$ , \*\* $P < 0.01$ , \*\*\* $P < 0.001$ .

We synthesized these probes through a minimal structural change and compared their properties, and investigated their response towards FA (Table S1 and Figure S1). The four-membered azetidine ring-substituted probe (FATP-1) exhibited an increased ratio of quantum yield value (>3 fold) compared to the corresponding fluorophore, which is similar to that of FATP-4. FATP-1 exhibited the most significant increase in fluorescence intensity (>6 fold) after reactivating with FA, suggesting that the azetidine ring-substitution can effectively mitigate the twisted internal charge transfer (TICT) and improve fluorescence brightness.<sup>22</sup> This significantly improved brightness of the fluorophore resulting from FATP-1 was also observed under two-photon excitation (Figure 1A and S2). The maximum two-photon absorption cross-section ( $\sigma_2$ ) values of  $78.44 \pm 2.89$  GM at 750 nm ( $\sim 3$  fold of enhancement), suggesting the suitability of FATP-1 for two-photon imaging. Importantly, this probe

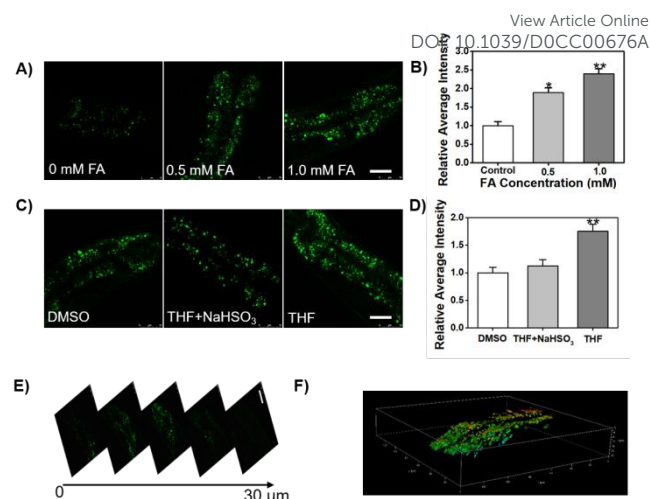


**Figure 2.** (A) Two-photon fluorescence images of *C. elegans*. *C. elegans* were pretreated with FA (0, 0.5, and 1 mM) at 20°C for 2 h, then *C. elegans* were washed and incubated with FATP-1 (20  $\mu\text{M}$ ) for another 30 min before imaging. Green channel: collected at 540–600 nm,  $\lambda_{\text{ex}}=750$  nm, scale bar = 25  $\mu\text{m}$ . (B) Quantification of the relative ratio of fluorescence intensity shown in (A). (C) *C. elegans* were pretreated with DMSO or THF, then NaHSO<sub>3</sub> or H<sub>2</sub>O at 20°C for 2 h, then washed and incubated with FATP-1 (20  $\mu\text{M}$ ) for another 30 min before imaging. Green channel: collected at 540–600 nm,  $\lambda_{\text{ex}}=750$  nm, scale bar = 25  $\mu\text{m}$ . (D) The relative ratio of fluorescence intensity shown in (C) was quantified. (E) Two-photon fluorescence images at different depths in *C. elegans*. *C. elegans* were pretreated with FA (1 mM) at 20°C for 2 h, then washed and incubated with FATP-1 (20  $\mu\text{M}$ ) for another 30 min before imaging. Green channel: collected at 540–600 nm,  $\lambda_{\text{ex}}=750$  nm, scale bar = 25  $\mu\text{m}$ . (F) Perspective for 3D image of (E). The error bars were  $\pm\text{SD}$  (n=3). Statistical analyses performed with an Ordinary one-way ANOVA test to the control with H<sub>2</sub>O or DMSO treatment, \* $P < 0.05$ , \*\* $P < 0.01$ .

displayed a robust fluorescence response to FA. Upon treatment with 2 mM FA, the fluorescence intensity enhanced dramatically in a time-dependent manner over 60 min and can reach a plateau after  $\sim 3$  h (Figure S3). The change of fluorescence is ascribed to uncaging of FATP-1, which was further confirmed by infrared spectroscopy (IR) and high performance liquid chromatography (HPLC) experiments (Figure S4–5 and Scheme S2). To test the response of FATP-1 under physiological conditions, the probe was exposed in different pH buffers from 3 to 12. A relatively wide range of pH applications was observed (Figure S6). Moreover, a concentration-dependent fluorescent enhancement was observed from 0 to 2 mM FA treatment (Figure 1B and S7), and the detection limit was calculated to be about 0.3  $\mu\text{M}$ . These findings suggest FATP-1 has the capability for detecting the intracellular FA (0.1–0.4 mM). To investigate the selectivity and anti-interference ability of FATP-1 towards FA, the fluorescence changes of FATP-1 were also observed in the presence of various other relevant species (Figure 1C and S8). We found that the strongest response towards FA, while negligible emission changes for other relevant aldehydes and bio-molecules. Besides, log  $P$  of FATP-1 was 2.43 in an octanol/water system. These observations demonstrate that FATP-1 can selectively respond to FA over other biological analytes under physiological conditions.

We next assessed the feasibility of using FATP-1 to detect FA in living cells. The cytotoxicity of the probe was first established using cell CCK-8 assays with human neuroblastoma SH-SY5Y cells, demonstrating negligible cytotoxicity of FATP-1 to live cells (Figure 1D). SH-SY5Y cells were incubated with FATP-1 (10  $\mu\text{M}$ ) for 30 min,

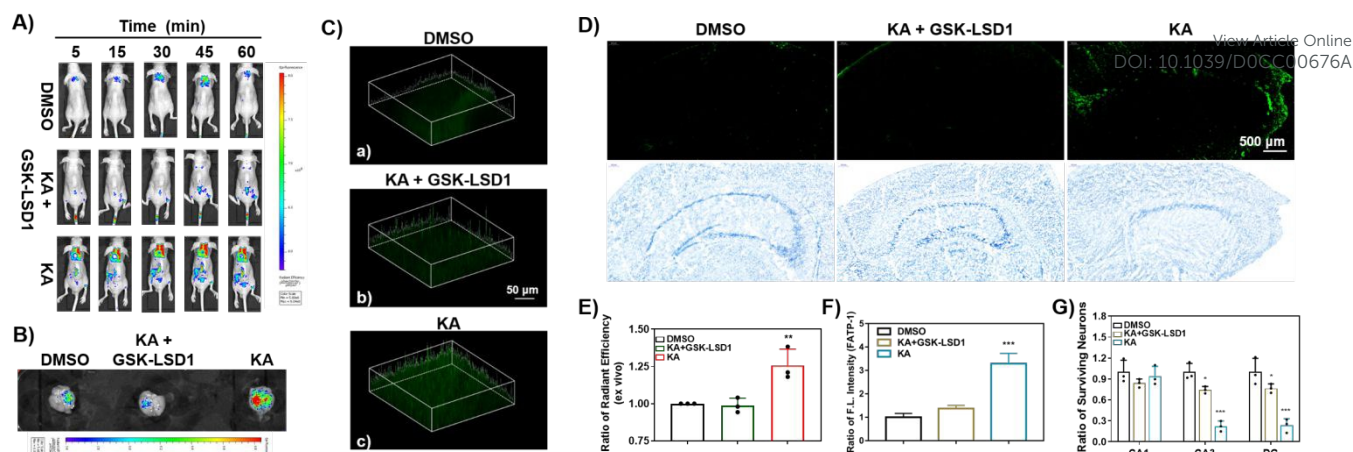


**Figure 3.** (A) Fluorescence images of three groups mice [wide-type (WT), combination KA with GSK-LSD1 and KA-induced epileptic mice] at 5, 15, 30, 45, and 60 min after *i.v.* injection with FATP-1 (0.5 mg/kg). KA (6 mg/kg, 12 h) was intraperitoneal (*i.p.*) injected into mouse to cause epilepsy. At the same time, GSK-LSD1 (0.15 mg/kg, 12 h) was intraperitoneal (*i.p.*) injected into mouse to inhibit the production of HCHO. (B) Ex vivo fluorescence images of relative HCHO levels in mice brains 60 min post-injection of FATP-1. (C) The two-photon fluorescence images of 2.5D volume-rendered and different depths of maximum hippocampal surface in brain tissues from (B). Green=FATP-1 channel. Fluorescence excitation filter MP 750 nm, emission filter 475-600 nm. Scale bar= 50  $\mu\text{m}$ . (D) Fluorescent imaging and Nissl's staining for evaluating neuronal damage in the whole hippocampal region (HIP), and CA1, CA3, dentate gyrus (DG) sub-regions after KA administration. Scale bar =500  $\mu\text{m}$ . (E) Quantification of images in (B). Note that fluorescence signals in KA-induced epileptic mice were significantly higher than those in the healthy WT group. Treatment with GSK-LSD1 would help to inhibit the overexpressed HCHO. (F) Quantification of images in (D). (G) Quantification of images of the CA1, CA3, and DG sub-regions of hippocampus in (D). The relative ratio of fluorescence intensity of the brains shown in A and B was quantified using the IVIS Spectrum imaging system. The data are expressed as the mean  $\pm$  S.D. (n=3). Statistical analyses performed with Ordinary one-way or two-way ANOVA test to the control with DMSO treatment, \* $P < 0.05$ , \*\* $P < 0.01$ , \*\*\* $P < 0.001$ .

then washed by PBS buffer three times to remove the excess probe. Flow cytometry analysis was performed after incubation with exogenous addition of FA (0-1 mM) for another 4 h (Figure 1E). A dose-dependent increase of fluorescence signal was clearly observed, suggesting excellent cell-membrane permeability and ability for FA detection in live cells. To further investigate the suitability of FATP-1 for detecting the stimuli-triggered dynamic changes of endogenous FA fluxes in live cells, cells were pretreated with different exogenous substances, their fluorescence intensities of cells were quantitatively analyzed by a flow cytometer (Figure 1F). Pretreatment with a high concentration of glutamate to stimulate cells,<sup>23</sup> a great fluorescence enhancement was observed. Similarly, preloading cells with kainic acid (KA),<sup>24</sup> a glutamate analog widely used as an epilepsy-inducing reagent,<sup>25</sup> an obvious increase in fluorescence signal was clearly observed, suggesting that intracellular FA levels increased under stimulation of external oxidative stress. To measure the endogenous FA as a result of metabolism, cells were pre-incubated with methanol (MeOH)<sup>26</sup> or tetrahydrofolate (THF),<sup>27</sup> a significant increase in fluorescence intensity was observed; while co-treated with sodium bisulfite (NaHSO<sub>3</sub>) as the FA scavenger,<sup>28</sup> cells showed a decrease in overall fluorescent intensity. These findings reveal that FATP-1 can be used as an efficient tool for determinate the endogenously generated FA from metabolic processes in live cells. Additionally, pretreatment with GSK-LSD1 or TCP (inhibitors of LSD1, lysine-specific histone demethylase 1A),<sup>29</sup> a decrease in fluorescence signal compared to control cells was observed, specifically GSK-LSD1 treated cells gives a more significant decrease than TCP treated cells, suggesting that the pharmacological inhibition of LSD1 decreased intracellular FA levels, an outcome probably associated with certain epigenetic modifications that can be revealed by using FATP-1.<sup>2</sup>

To examine whether FATP-1 could function in vivo, we initially use FATP-1 to monitor FA in live *C. elegans*. After exposing *C. elegans*

with exogenous FA (0, 0.5, and 1 mM) at 20°C for 2 h, *C. elegans* were washed and incubated with FATP-1 (20  $\mu\text{M}$ ) for another 30 min. Two-photon fluorescence imaging showed a dose-dependent enhancement for FA (Figure 2A and B). To directly detect endogenous FA fluxes that generated through THF metabolism in vivo, *C. elegans* were pretreated with either DMSO or THF, water or NaHSO<sub>3</sub>, and then incubated with FATP-1 (20  $\mu\text{M}$ ) for another 30 min (Figure 2C and D). A significant difference between THF and negative control group was observed, which is consistent with the flow cytometry analytic results in live cells. However, we did not observe any statistically obvious difference between the group that was incubated with both THF and the FA scavenger NaHSO<sub>3</sub> and the negative control group, further confirming the enhanced fluorescence of *C. elegans* was caused by endogenous FA resulting from THF metabolism in vivo. Additionally, to test the depth TP imaging capability of FATP-1, images of *C. elegans* were observed under two-photon excitation at 750 nm (Figure 2E and F). We can clearly observe the 3D images of the live *C. elegans* in the whole depth, revealing the great potential of FATP-1 for deep tissue TP imaging.

To further investigate of the feasibility of using FATP-1 to study the influence of external stimuli on FA generation in vivo, *C. elegans* were pre-exposed with 10% MeOH for 2 h, TP images were observed after incubation with FATP-1 for another 30 min (Figure S9A and B). An increase in the TP fluorescence signal was observed, suggesting the metabolism of MeOH can induce the increased level of FA in vivo. In addition, we also observed that the exogenous supplement of Fenton-reaction substrates including iron ions and hydrogen peroxide led to increased endogenous FA generation in vivo. Compared with the control *C. elegans*, Glu/KA-treated *C. elegans* exhibited significantly enhanced TP fluorescence (Figure S9C and D). Interestingly, pretreatment with H<sub>2</sub>S can decrease the fluorescence signal of *C. elegans*, suggesting that H<sub>2</sub>S might downregulate the

generation of endogenous FA. Since excessive expression of cellular LSD1 has been implicated in the abnormally elevated endogenous FA, we further assessed whether FATP-1 can be used for monitoring the fluctuations of the endogenous FA caused by the epigenetic regulation of LSD1 activity in vivo. Live *C. elegans* that pre-incubated with LSD1 inhibitors exhibit weaker TP fluorescence signals (Figure S10), indicating that down-regulation of LSD1 activities can efficiently regulate the generation of endogenous FA in vivo. Taken together, these observations confirm that FATP-1 can effectively monitor fluctuations of endogenous FA under various external stimuli in vivo.

Finally, we assessed FATP-1 as a TP imaging probe in the live animal brain, especially in the epileptic brain. Wild-type mice were performed direct intraperitoneal (*i.p.*) injection of KA (6 mg/Kg) to establish the classical epilepsy animal model.<sup>30</sup> Mice were then injected (*i.p.*) with either DMSO or GSK-LSD1 for 12 h, followed by intravenous (*i.v.*) injection of FATP-1 (0.5 mg/kg). The in vivo and ex vivo fluorescence images of mice brains were obtained with an IVIS imaging system every 15 min over a 60 min period (Figure 5A and B). We observed a significant increase of fluorescence in KA-induced epileptic brains, while co-treatment with GSK-LSD1 led to little difference in fluorescence signal compared to that of the wild-type (WT) healthy mice. These data demonstrated the capability of FATP-1 in BBB penetration and tracing the dynamic changes of FA levels in the live epileptic brain. The frozen tissue sections from these mice brains exhibited significantly increased fluorescence in the cerebral cortex regions of KA-induced epileptic brains compared with the negative control (Figure 3C-D and S11-12). In agreement with these in vivo and ex vivo imaging results (Figure 3E and S13), the co-treatment with GSK-LSD1 effectively decreased the fluorescence in the epileptic brain tissues (Figure 3F). These observations indicate that the pathological process of epilepsy is accompanied by an abnormal elevation of FA level and neuronal damage in the brain (Figure 3G), inhibition of abnormally elevated endogenous FA could help to alleviate neuronal damage in the epileptic brain.

In conclusion, we have reported the first two-photon fluorescence probe for imaging endogenous FA fluxes in live cells, animals and brain tissues. The unique quinoline skeleton in these probes led to excellent BBB permeability and two-photon properties. Functionalization at the electron-donor group with a four-membered azetidone group yields a new generation of FA probes with improved brightness and photostability. The use of the 2-aza-Cope FA reactive trigger has ensured the selectivity of the probes towards FA, as well as their cellular permeability. In vivo studies revealed a significant increase in endogenous FA levels in live cells and *C. elegans* under oxidative stress. Importantly, fluctuations of endogenous FA in the epileptic mouse brains were successfully monitored by TP fluorescence imaging, suggesting a correlation between the abnormally elevated FA levels in the brain and the epilepsy phenotype. This work provides a robust chemical tool for probing endogenous FA in vivo and might be used in the further to give crucial information for the prevention and treatment of FA-related neurodegenerative disease.

This work is financially supported by the National Natural Science Foundation of China (21778033), the program of Jiangsu Specially-Appointed Professor for Y.Q., the Science and Technology Innovation Project of Nanjing (184080H201136),

and the Open Project of State Key Laboratory of Pharmaceutical Biotechnology (KF-GN-202002). DOI: 10.1039/D0CC00676A

## Conflicts of interest

There are no conflicts to declare.

## Notes and references

- R. He, J. Lu and J. Miao, *Sci China Life Sci*, 2010, **53**, 1399-1404.
- Y. Shi, F. Lan, C. Matson, P. Mulligan, J. R. Whetstone, P. A. Cole, R. A. Casero and Y. Shi, *Cell*, 2004, **119**, 941-953.
- J. O'Sullivan, M. Unzeta, J. Healy, M. I. O'Sullivan, G. Davey and K. F. Tipton, *Neurotoxicology*, 2004, **25**, 303-315.
- M. E. Andersen, H. J. Clewell, 3rd, E. Bermudez, D. E. Dodd, G. A. Willson, J. L. Campbell and R. S. Thomas, *Toxicol Sci*, 2010, **118**, 716-731.
- Z. Tong, C. Han, W. Luo, X. Wang, H. Li, H. Luo, J. Zhou, J. Qi and R. He, *Age (Dordr)*, 2013, **35**, 583-596.
- Z. Tong, W. Luo, Y. Wang, F. Yang, Y. Han, H. Li, H. Luo, B. Duan, T. Xu, Q. Maoying, H. Tan, J. Wang, H. Zhao, F. Liu and Y. Wan, *PLoS One*, 2010, **5**, e10234.
- M. Unzeta, M. Sole, M. Boada and M. Hernandez, *J Neural Transm (Vienna)*, 2007, **114**, 857-862.
- J. Lu, J. Miao, T. Su, Y. Liu and R. He, *Biochim Biophys Acta*, 2013, **1830**, 4102-4116.
- K. Tulpule and R. Dringen, *J Neurochem*, 2013, **127**, 7-21.
- J. S. Hu, C. Shao, X. Wang, X. Di, X. Xue, Z. Su, J. Zhao, H. L. Zhu, H. K. Liu and Y. Qian, *Adv Sci (Weinh)*, 2019, **6**, 1900341.
- A. Roth, H. Li, C. Anorma and J. Chan, *J Am Chem Soc*, 2015, **137**, 10890-10893.
- Z. Li, Y. Xu, H. Zhu and Y. Qian, *Chem Sci*, 2017, **8**, 5616-5621.
- M. Gao, F. Yu, C. Lv, J. Choo and L. Chen, *Chem Soc Rev*, 2017, **46**, 2237-2271.
- Z. Lou, P. Li and K. Han, *Acc Chem Res*, 2015, **48**, 1358-1368.
- J. Ning, W. Wang, G. B. Ge, P. Chu, F. D. Long, Y. L. Yang, Y. L. Peng, L. Feng, X. C. Ma and T. D. James, *Angew Chem Int Edit*, 2019, **58**, 13618-13618.
- Q. Li, J. S. Lee, C. Ha, C. B. Park, G. Yang, W. B. Gan and Y. T. Chang, *Angew Chem Int Ed Engl*, 2004, **43**, 6331-6335.
- M. Chioua, E. Martinez-Alonso, R. Gonzalo-Gobernado, M. I. Ayuso, A. Escobar-Peso, L. Infantes, D. Hadjipavlou-Litina, J. J. Montoya, J. Montaner, A. Alcazar and J. Marco-Contelles, *J Med Chem*, 2019, **62**, 2184-2201.
- Z. Mao, L. Hu, X. Dong, C. Zhong, B. F. Liu and Z. Liu, *Anal Chem*, 2014, **86**, 6548-6554.
- J. Ohata, K. J. Bruemmer and C. J. Chang, *Acc Chem Res*, 2019, **52**, 2841-2848.
- T. F. Brewer and C. J. Chang, *J Am Chem Soc*, 2015, **137**, 10886-10889.
- J. B. Grimm, B. P. English, J. Chen, J. P. Slaughter, Z. Zhang, A. Revyakin, R. Patel, J. J. Macklin, D. Normanno, R. H. Singer, T. Lionnet and L. D. Lavis, *Nat Methods*, 2015, **12**, 244-250, 243 p following 250.
- J. B. Grimm, B. P. English, H. Choi, A. K. Muthusamy, B. P. Mehl, P. Dong, T. A. Brown, J. Lippincott-Schwartz, Z. Liu, T. Lionnet and L. D. Lavis, *Nat Methods*, 2016, **13**, 985-988.
- D. W. Choi, *Neuron*, 1988, **1**, 623-634.
- L. Silayeva, T. Z. Deeb, R. M. Hines, M. R. Kelley, M. B. Munoz, H. H. Lee, N. J. Brandon, J. Dunlop, J. Maguire, P. A. Davies and S. J. Moss, *Proc Natl Acad Sci U S A*, 2015, **112**, 3523-3528.
- M. Levesque and M. Avoli, *Neurosci Biobehav R*, 2013, **37**, 2887-2899.
- A. V. Shindyapina, T. V. Komarova, E. V. Sheshukova, N. M. Ershova, V. N. Tashlitsky, A. V. Kurkin, I. R. Yusupov, G. V. Mkrtchyan, M. Y. Shagidulin and Y. L. Dorokhov, *Front Neurosci*, 2017, **11**, 651.
- G. Burgos-Barragan, N. Wit, J. Meiser, F. A. Dingler, M. Pietzke, L. Mulderrig, L. B. Pontel, I. V. Rosado, T. F. Brewer, R. L. Cordell, P. S. Monks, C. J. Chang, A. Vazquez and K. J. Patel, *Nature*, 2017, **548**, 549-554.
- K. J. Bruemmer, O. Green, T. A. Su, D. Shabat and C. J. Chang, *Angew Chem Int Ed Engl*, 2018, **57**, 7508-7512.
- M. G. Lee, C. Wynder, D. M. Schmidt, D. G. McCafferty and R. Shiekhattar, *Chem Biol*, 2006, **13**, 563-567.
- J. A. Miller, K. A. Kirkley, R. Padmanabhan, L. P. Liang, Y. H. Raol, M. Patel, R. A. Bialecki and R. B. Tjalkens, *Neurotoxicology*, 2014, **44**, 39-47.